

## Oxygen and rare-earth doping of the 90-K superconducting perovskite $\text{YBa}_2\text{Cu}_3\text{O}_{7-x}$

J. M. Tarascon, W. R. McKinnon,\* L. H. Greene, G. W. Hull, and E. M. Vogel  
*Bell Communications Research, 331 Newman Springs Road, Red Bank, New Jersey 07701-7020*  
 (Received 21 April 1987)

Structural, magnetic, and electronic properties of compounds in the series  $R\text{Ba}_2\text{Cu}_3\text{O}_{7-x}$  ( $R = \text{Nd, Sm, \dots, and Lu}$ ) were studied. Resistivity, Meissner-effect, and shielding measurements have revealed superconductivity among all the rare-earth compounds, except La, Pr, and Tb, with critical temperatures  $T_c$  measured at the midpoint of the resistive transition ranging from 87 to 95 K. No depression of  $T_c$  was observed upon introduction of most of the rare-earth magnetic ions. Susceptibility measurements down to 1.6 K have shown that an antiferromagnetic ordering (most likely due to dipole-dipole interactions) occurs only for the Gd compound. Changes in oxygen content in these materials drastically affect their physical properties. The importance of the cooling rate during the synthesis of the sample has been correlated to oxygen content.  $T_c$ 's are optimized by slow cooling. Annealing at 700°C in oxygen pressure of 40 atmospheres slightly increases  $T_c$ , while annealing under vacuum at 420°C destroys  $T_c$  and induces a semiconducting behavior. These changes in oxygen content and  $T_c$  are perfectly reversible.

### INTRODUCTION

The recent discovery of superconductivity at 30 K in the Ba-La-Cu-O system by Bednorz and Müller<sup>1</sup> has generated tremendous interest among physicists and material scientists and sparked intensive studies of the cuprate systems. Superconductivity in the above system was ascribed to the oxygen-defect perovskite phase  $\text{La}_{2-x}\text{Ba}_x\text{CuO}_4$  (Refs. 2 and 3) and within the same system bulk superconductivity at 40 K has been established by other workers using strontium instead of barium as doping.<sup>4-6</sup> Further research has led Wu *et al.*<sup>7</sup> to the discovery of superconductivity at 90 K in the multiphase Y-Ba-Cu-O system. We independently confirmed their results,<sup>8</sup> isolated the phase ( $\text{YBa}_2\text{Cu}_3\text{O}_{7-x}$ ) responsible for superconductivity in this system, and established its crystal structure.<sup>9</sup> The structure can be viewed (Fig. 1) as a stacking of three perovskite layers with a plane of yttrium atoms every three layers. Independently, this phase was also isolated by two other research groups.<sup>10,11</sup> The  $\text{YBa}_2\text{Cu}_3\text{O}_{7-x}$  phase is deficient in oxygen, but x-ray crystallography could not provide evidence for the ordering of the oxygen vacancies. However, recent neutron studies<sup>12</sup> have unambiguously shown that the oxygen vacancies are ordered, leading to the presence of copper-oxygen chains within the structure.

Our previous studies<sup>6</sup> of the La-Sr-Cu-O perovskite have shown that  $T_c$  is dramatically affected by subtle changes in oxygen content. Here we show that oxygen plays an important role in the Y-Ba-Cu-O system as well.

An exciting challenge is to understand the interplay between magnetism and superconductivity. This was addressed in our study of the substitution of La by other rare-earth metals in the 40 K superconducting phase.<sup>13</sup> In those materials, we found that increasing the concentration of rare-earth  $R$  ions depressed  $T_c$ , probably due to a volume-change effect. However, a magnetic ordering transition was never observed because the phase was destroyed before a sufficient concentration of magnetic ions could be added. We have performed similar studies with

the 90-K superconducting  $\text{YBa}_2\text{Cu}_3\text{O}_{7-x}$  phase and find that the compounds  $R\text{Ba}_2\text{Cu}_3\text{O}_{7-x}$  ( $R = \text{Sm, Eu, Gd, Dy, Ho, Er, Tm}$ ) can be prepared as single phase and that the  $T_c$  for these phases remains essentially constant at  $93 \pm 2$  K, independent of  $R$ . None of these phases order magnetically down to 1.6 K, except  $\text{GdBa}_2\text{Cu}_3\text{O}_{7-x}$  which orders antiferromagnetically at  $T_N = 2.3$  K. During the course of

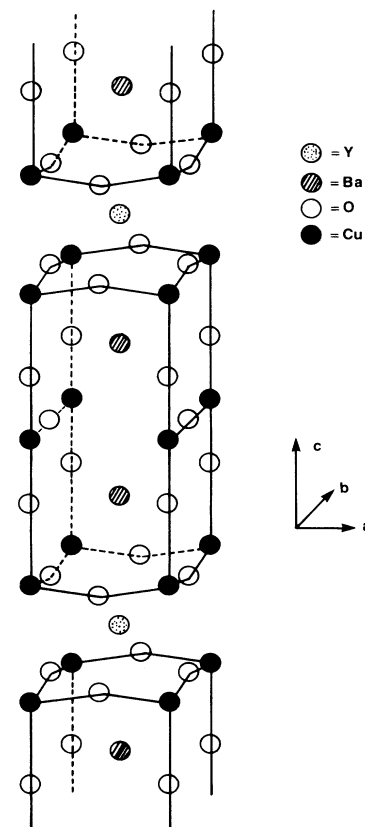


FIG. 1. The structure of  $\text{YBa}_2\text{Cu}_3\text{O}_{7-x}$  is shown.

this investigation, we learned of work by Fisk *et al.*<sup>14</sup> and Takagi *et al.*<sup>15</sup> who have investigated the  $R$  substitution on mixed-phase materials and by Murphy *et al.*,<sup>16</sup> who have intensively studied the  $\text{EuBa}_2\text{Cu}_3\text{O}_{7-x}$  phase.

### EXPERIMENT

Samples of nominal composition  $\text{RBa}_2\text{Cu}_3\text{O}_{7-x}$  ( $R$ =rare earth) were prepared by thoroughly mixing appropriate amounts of  $\text{BaCO}_3$ ,  $\text{R}_2\text{O}_3$ , and  $\text{CuO}$  powders, each 99.999% pure. For reasons of simplicity, in the following  $R$  will also refer to yttrium. The mixed powders were packed into alumina crucibles and placed in a tubular furnace. The samples were heated up to  $960^\circ\text{C}$  in air in 10 h, maintained at this temperature for 72 h, then cooled in 2 h to  $300^\circ\text{C}$ , then removed from the furnace. The resulting materials were crystallized, sparkling black powders. A part of each sample was kept aside to select single crystals for x-ray studies and the other part was ground, pressed into a  $\frac{1}{2}$ -in.-diam pellet, reannealed under oxygen at  $950^\circ\text{C}$  for 2 days, and cooled in 2 h. We found that the cooling rate strongly affects the physical properties of the samples. Finally, the pellets were cut in rectangular bars ( $0.5 \times 3 \times 8 \text{ mm}^3$ ) for resistivity measurements and the remainder was ground for powder x-ray diffraction, thermogravimetric analysis (TGA), and magnetic-susceptibility measurements.

The crystal structure<sup>9</sup> has revealed that these compounds contain oxygen defects. Therefore, one might expect that like the  $\text{La}_{2-x}\text{Sr}_x\text{CuO}_4$  system, the oxygen content can be increased or decreased by annealing the samples under oxygen or vacuum, respectively. We annealed some of the samples at  $720^\circ\text{C}$  under 40 bars of oxygen or at  $420^\circ\text{C}$  under vacuum ( $10^{-3}$  Torr), and remeasured their physical properties. The oxygen stoichiometry in the as-prepared sample was determined by thermogravimetric analysis in which the weight loss of a sample heated at  $20^\circ\text{C}/\text{min}$  in a reducing atmosphere (4%  $\text{H}_2$  in Ar) was monitored. The oxygen content was calculated by assuming that the reduction products are  $\text{R}_2\text{O}_3$ ,  $\text{BaO}$ , and  $\text{Cu}$  metal. The oxygen content for the vacuum-annealed samples was indirectly determined by TGA, from the increase in weight of the samples heated at  $20^\circ\text{C}/\text{min}$  in an  $\text{O}_2$  atmosphere.

Resistivities were measured using a standard four-probe method on samples with silver paint contacts. In some samples, the contacts were removed with acetone so the sample could be reannealed and remeasured. The shielding currents, the Meissner-effect expelled flux, and the susceptibility from 4.2 K to room temperature were measured with a superconducting quantum interference device magnetometer. The thermometers used in both resistivity and susceptibility measurements were calibrated to  $\pm 0.2$  K. The samples were characterized by powder x-ray diffraction in the Bragg-Brentano geometry with  $\text{Cu K}\alpha$  radiation.

### RESULTS

X-ray powder diffraction shows that the compounds of nominal composition  $\text{RBa}_2\text{Cu}_3\text{O}_{7-x}$  with  $R=\text{Sm}$ ,  $\text{Gd}$ ,  $\text{Eu}$ ,  $\text{Dy}$ ,  $\text{Ho}$ ,  $\text{Er}$ , and  $\text{Tm}$  are single phase. The materials

with  $R=\text{La}$ ,  $\text{Pr}$ ,  $\text{Nd}$ , and  $\text{Yb}$  have weak extra peaks corresponding to a few percent of a second unidentified phase; for  $R=\text{Lu}$ , the second phase accounted for at least half the intensity in the powder pattern, and we could not reliably refine the lattice parameters. The compound with  $R=\text{Tb}$  did not form under the conditions described above, even though its neighboring compounds with  $\text{Gd}$  and  $\text{Dy}$  formed easily. Perhaps this is because  $\text{Tb}$  can

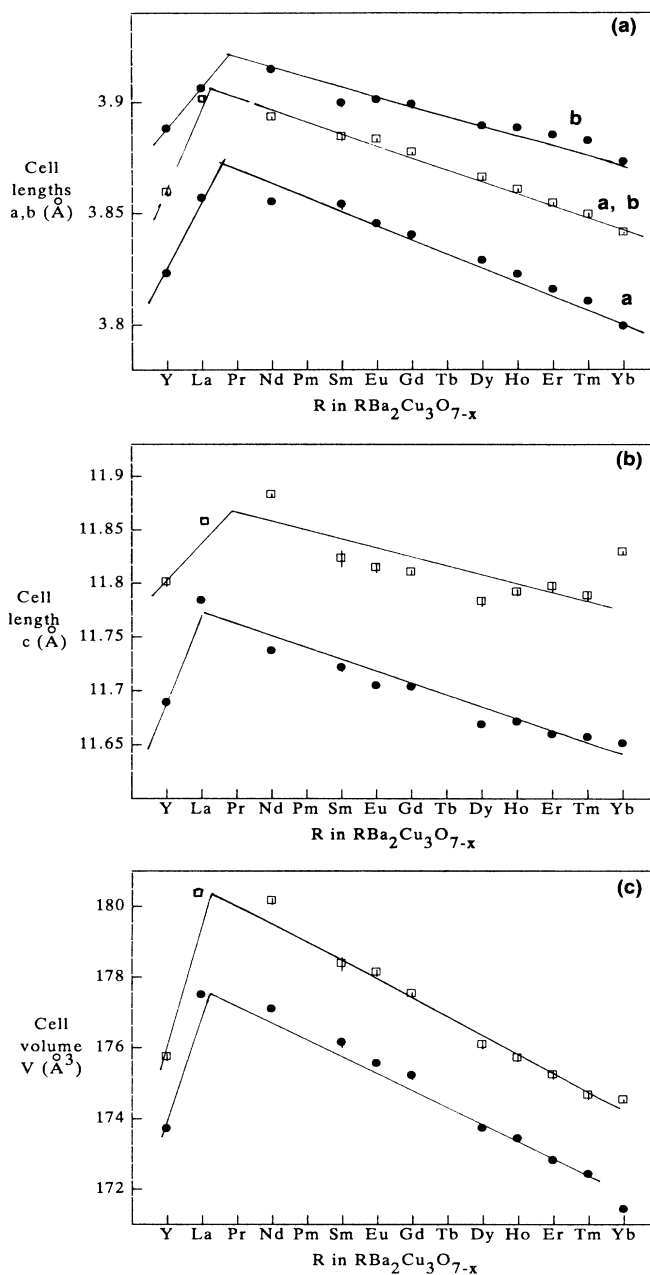


FIG. 2. Orthorhombic unit cell parameters ( $a, b, c, V$ ) as a function of the rare earth  $R$  in the  $\text{RBa}_2\text{Cu}_3\text{O}_{7-x}$  series for the as-prepared samples (filled circles) and vacuum-annealed samples (open squares) are shown. The lines drawn are a guide to the eye.

TABLE I. Lattice parameters for  $RBa_2Cu_3O_{7-x}$ ,  $R=Y$ , or a rare-earth element, for compounds as prepared under 1 atm  $O_2$  (orthorhombic) or annealed under vacuum (tetragonal). The oxygen content  $x$  in the samples as prepared and the change in oxygen  $\Delta x$  after annealing in vacuum are measured with TGA as described in the text.  $a$ ,  $b$ ,  $c$  are the lengths of edges of the unit cell, and  $V$  is the volume of the unit cell. Numbers in parentheses are twice the standard deviation of the last digit. The parameters for Pr are those for a cubic refinement of the dominant peaks in the powder pattern, as described in the text.

$R$	$x$	As prepared (under $O_2$ )				$\Delta x$	Annealed under vacuum		
		$a$ (Å)	$b$ (Å)	$c$ (Å)	$V$ (Å <sup>3</sup> )		$a, b$ (Å)	$c$ (Å)	$V$ (Å <sup>3</sup> )
Y	6.72	3.8237(8)	3.8874(8)	11.657(2)	173.28(6)	0.53	3.8589(8)	11.800(4)	175.72(10)
La		3.8562(8)	3.9057(10)	11.783(3)	177.47(7)		3.9007(8)	11.858(3)	180.42(9)
Pr		3.922(2)			180.87(11)/3				
Nd	7.16	3.8546(8)	3.9142(12)	11.736(2)	177.07(7)	0.69	3.8930(6)	11.882(2)	180.13(9)
Sm	7.11	3.855(2)	3.899(2)	11.721(4)	176.11(13)	0.47	3.884(2)	11.822(8)	178.4(2)
Eu	7.10	3.8448(8)	3.9007(10)	11.704(3)	175.53(7)	0.51	3.8829(8)	11.814(4)	178.11(10)
Gd	7.08	3.8397(12)	3.8987(18)	11.703(3)	175.19(11)	0.56	3.8770(6)	11.810(2)	177.51(6)
Dy	6.82	3.8284(8)	3.8888(8)	11.668(2)	173.71(5)	0.54	3.8656(10)	11.783(5)	176.07(11)
Ho	6.71	3.8221(8)	3.8879(8)	11.670(2)	173.42(6)	0.58	3.8601(8)	11.791(3)	175.69(9)
Er	6.82	3.8153(8)	3.8847(12)	11.659(2)	172.80(7)	0.66	3.8540(8)	11.796(4)	175.22(11)
Tm	6.65	3.8101(8)	3.8821(12)	11.656(2)	172.41(7)	0.58	3.8491(10)	11.788(4)	174.65(10)
Yb	6.71	3.7989(8)	3.8727(10)	11.650(2)	171.40(6)	0.70	3.8411(4)	11.828(2)	174.51(5)

have two oxidation states (3+ and 4+), as indicated by the starting oxide  $Tb_4O_7$ .

Figure 2 and Table I give the lattice parameters for samples annealed in oxygen at 950 °C and annealed under vacuum at 420 °C. (For  $R=Pr$ , the peaks overlap strongly, suggesting  $a$ ,  $b$ , and  $c/3$  are all about equal to a refined value of 3.922.) The samples annealed under oxygen are orthorhombic, but  $c/3$  is almost equal to  $b$ , so many of the peaks overlap in the powder pattern;  $a$  is about 2% smaller than  $b$  or  $c/3$ . Annealing one sample (Y) under 40 atm of oxygen did not change  $a$  or  $b$  within experimental error, but did reduce  $c$  by 0.3%.

When the samples are annealed under vacuum they become tetragonal to within our resolution. The parameter  $c$  increases by about 1%, and  $a$  and  $b$  become equal to a value slightly larger than the average of their values in the samples annealed under oxygen;  $c/3$  is about 2% longer than  $a$  and  $b$ . In the oxygen-annealed samples, the oxygen in the Cu-O layer between adjacent Ba layers is ordered; oxygen occupies sites joining Cu atoms along the long direction  $b$  but not along the shorter direction  $a$ .<sup>12</sup> For the structure to become tetragonal, the oxygen must be disordered, so either sites along both  $a$  and  $b$  must be occupied or else both must be empty. All the lattice parameters vary smoothly across the rare-earth series except  $c$  in the vacuum-annealed samples, which has a minimum near Tb, the only member of the series which we could not prepare.

The two compounds  $R=Pr$  and La are not superconducting. The powder pattern of Pr is almost cubic, and the  $a$  parameter is about 0.7% larger than expected from the average parameters of the neighboring compounds La and Nd. The compound with  $R=La$  appears in line with the others, but it shows the smallest change in  $c$  on annealing in vacuum, and  $a$  for the vacuum-annealed sample is almost equal to  $b$  for the compound prepared in oxygen. These differences for  $R=Pr$  and La suggest that the arrangement or concentration of oxygen in these compounds is different from the other members of the series, and

perhaps that is why they are not superconducting.

The rare-earth samples were reduced under an argon-hydrogen mixture to determine the oxygen content. The TGA traces obtained for  $YBa_2Cu_3O_{7-x}$  are shown in Fig. 3. A value of 6.72 for the oxygen content was obtained assuming the end products are Cu, BaO, and  $Y_2O_3$ , which is in reasonable agreement with 6.7, obtained from recent neutron studies. However, caution has to be exercised in so interpreting the data because of several problems. First, it is difficult to determine the final temperature on the TGA curve at which the reduction process is completed. Second, powder x-ray diffraction of the reduced product for the Y compound indicates several peaks from BaO and Cu metal but only one from  $Y_2O_3$ . The formation of  $Y_2Cu_2O_5$  instead of  $Y_2O_3$  has even been suggested,<sup>12</sup> but we were not able to detect evidence for this phase by powder x-ray diffraction. Thus our calculations were performed using BaO,  $Y_2O_3$ , and Cu metal as reduction

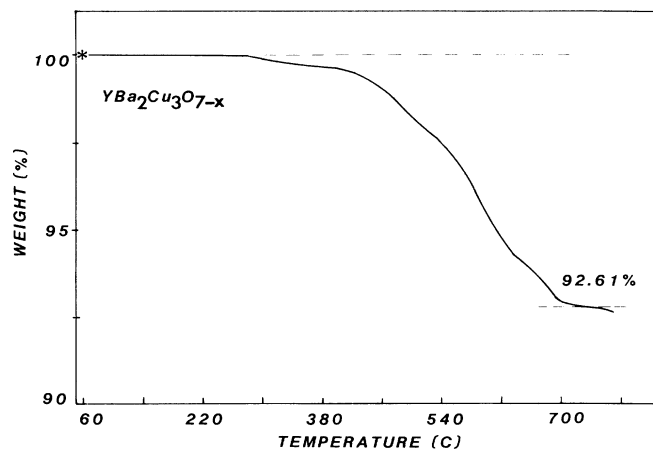


FIG. 3. Oxygen content in  $YBa_2Cu_3O_{7-x}$  determined by thermogravimetric analysis in argon-hydrogen mixture.

products. The TGA results are summarized in Table I. The oxygen content changes nonsystematically between 6.7 and 7.1.

The loss in oxygen for the rare-earth samples during their annealing at 420 °C under vacuum was determined by reannealing them under oxygen and measuring the increase in weight by TGA. A TGA trace is reported in Fig. 4(a) for  $\text{YBa}_2\text{Cu}_3\text{O}_{7-x}$ . On heating, the weight increase in oxygen becomes maximum at 500 °C and then decreases. On cooling in oxygen (20 °C/min), the curve follows the heating curve above 500 °C, indicating reversible intercalation over this temperature range. Below 500 °C, however, the cooling curve deviates from the heating one with a slight increase, indicating that the sample is further taking oxygen on cooling. The changes in oxygen stoichiometry ( $\Delta x$ ) of the vacuum-annealed rare-earth samples, deduced from the difference in sample weight between 50 °C and the temperature at which the TGA trace exhibits a maximum, are listed in Table I. The value of  $\Delta x$  is underestimated by as much as 10% because the sample takes additional oxygen on cooling. For example, by taking the weight of the yttrium sample after cooling, we obtained a  $\Delta x$  of 0.6 instead of 0.53. For the rare-earth series  $\Delta x$  lies between 0.5 to 0.7 per unit formula leading to compounds of general formula  $\text{RBa}_2\text{Cu}_3\text{O}_{7-x}$  ( $0.6 \leq x \leq 1$ ). This formula implies an average valence of copper lower than 2, suggesting the formation of  $\text{Cu}^{1+}$  during the reduction process.

The vacuum-annealing experiments can be mimicked by heating the samples under a flow of argon. In that case, the loss in oxygen can directly be followed as a function of temperature by thermogravimetric analysis. Figure 4(b) shows the TGA traces for  $\text{YBa}_2\text{Cu}_3\text{O}_{7-x}$ . Note again the loss in oxygen of this material on heating up to 800 °C. This loss is higher than the loss caused by annealing at 420 °C under vacuum, 1.86% ( $\Delta x = 0.81$ ) instead of 1.23% ( $\Delta x = 0.53$ ), respectively, indicating that kinetics govern the deintercalation of oxygen in these phases at 420 °C. The sample was then cooled down to room tem-

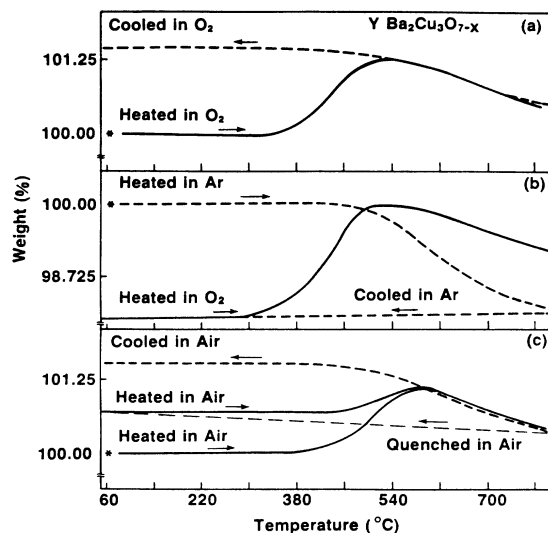


FIG. 4. The TGA traces are shown for  $\text{YBa}_2\text{Cu}_3\text{O}_{7-x}$  when heated and cooled in different partial pressures of oxygen. Each treatment sequence can simply be visualized by first looking at the star (starting point) and following the arrows. (a) A vacuum-annealed sample is first heated and then cooled under oxygen at a rate of 10 °C/min. (b) The as-prepared sample is heated under argon, cooled in argon and reheated in oxygen. (c) Finally a vacuum-annealed sample is heated in air, quenched in air, reheated in air and slow cooled in air.

perature and reannealed under oxygen. The material converts to its initial oxygen stoichiometry indicating a reversible intercalation of oxygen.

The importance of the cooling rate on the oxygen stoichiometry of the resulting material is illustrated in Fig. 4(c). Here  $\text{YBa}_2\text{Cu}_3\text{O}_{7-x}$  (vacuum annealed) was reannealed in air. The TGA curve shows, as previously, a peak at  $\approx 500$  °C. The amplitude of this peak is smaller than when pure oxygen is used, indicating the importance

TABLE II. The magnetic properties (Meissner, magnetic effective moments, and paramagnetic Curie temperatures) are reported for the  $\text{RBa}_2\text{Cu}_3\text{O}_{7-x}$  series, along with their electrical properties (resistivity and transition temperatures). The midpoint ( $T_{cm}$ ) of the superconducting transition is defined as described in the text.

Compounds	Meissner effect		$\mu_{\text{eff}}$ (expt)	$\Theta_p$	$T_{cm}$	$T_{C_{R=0}}$	$\rho(300)$ ( $\mu\Omega\text{cm}$ )
	(%)	$\mu_{\text{eff}}$ (theor)					
$\text{NdBa}_2\text{Cu}_3\text{O}_{7-x}$	48	3.62	...	...	95.3	92.0	4200
$\text{SmBa}_2\text{Cu}_3\text{O}_{7-x}$	32	0.85	...	...	93.5	88.3	2800
$\text{EuBa}_2\text{Cu}_3\text{O}_{7-x}$	35	0	...	...	94.9	93.7	2500
$\text{GdBa}_3\text{Cu}_3\text{O}_{7-x}$	36	7.94	7.75, 7.85 <sup>a</sup>	-2, -3 <sup>a</sup>	93.8	92.2	1650
$\text{DyBa}_2\text{Cu}_3\text{O}_{7-x}$	31	10.65	10.45, 10.69 <sup>a</sup>	-7, -8 <sup>a</sup>	92.7	91.2	1550
$\text{HoBa}_2\text{Cu}_3\text{O}_{7-x}$	33	10.61	10.48, 10.60 <sup>a</sup>	-16, -19 <sup>a</sup>	92.9	92.2	1200
$\text{ErBa}_2\text{Cu}_3\text{O}_{7-x}$	34	9.58	9.93, 9.63 <sup>a</sup>	-15, -16 <sup>a</sup>	92.4	91.5	1880
$\text{TmBa}_2\text{Cu}_3\text{O}_{7-x}$	33	7.56	7.53, 7.69 <sup>a</sup>	-35, -38 <sup>a</sup>	92.5	91.2	1110
$\text{YbBa}_2\text{Cu}_3\text{O}_{7-x}$	49	4.54	...	...	87.0	85.6	1000
$\text{LuBa}_2\text{Cu}_1\text{O}_{7-x}$	10	0	...	...	89.5	88.2	17000
$\text{YBa}_2\text{Cu}_3\text{O}_{7-x}$	35	...	...	...	93.4	91.5	2500

<sup>a</sup>Samples annealed under vacuum.

of the oxygen partial pressure in obtaining materials rich in oxygen. The sample was then quenched to room temperature. Because of the experimental setup we were not able to collect the TGA trace, but the weight of the sample after quenching was lower than it was when previously heated in air at 500°C. The quenched sample was then reannealed in air up to 800°C and slowly cooled (10°C/min) in air. A weight gain is observed during heating, and the sample gained further weight on cooling in air. The difference in oxygen stoichiometry between the sample after slow cooling and after quenching is large, 0.3. This clearly emphasizes the importance of the cooling rate on the synthesis of these materials. In a forthcoming paper, we correlate the oxygen content in these materials to their superconducting properties.<sup>17</sup>

The resistivity of the rare-earth samples from room temperature to below  $T_c$  is shown in Fig. 5. Note the linearity above  $T_c$  as observed also in the La-Sr-Cu-O system.<sup>6</sup> There is a general tendency for the room-temperature resistivity to decrease with the volume of the unit cell. This trend, however, could be fortuitous, and simply a result of the preparation procedure. The compounds with the largest resistivities, Nd and Lu, are contaminated by a second phase; it is possible that all the materials have some contamination, and that the degree of contamination varies systematically across the series. The midpoints of the resistive transitions lie between 92 and 95 K, except for those of Yb and Lu which are at 87 and 89.5 K, respectively. The shapes of the superconducting transitions are shown in more detail in Fig. 5. A remarkable feature is that most of the transition widths, when determined from 10% and 90% of the extrapolated high-temperature value, are less than 1 K. With increasing current, the superconducting transition shifts toward low temperatures, and the lower part of the transition broadens, developing a "resistive foot" like that seen for Sm in Fig. 6. This suggests small values for the critical

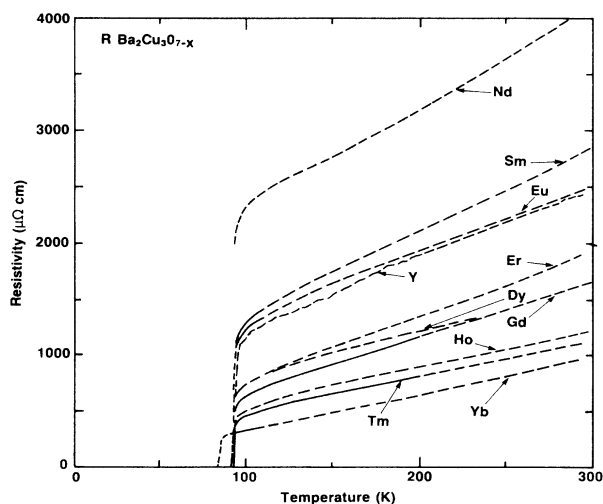


FIG. 5. Resistivity vs temperature from 300 K to below  $T_c$  for the  $R\text{Ba}_2\text{Cu}_3\text{O}_{7-x}$  series. Note the linear temperature dependence above  $T_c$ . Current densities were approximately 0.5 A/cm.<sup>2</sup>

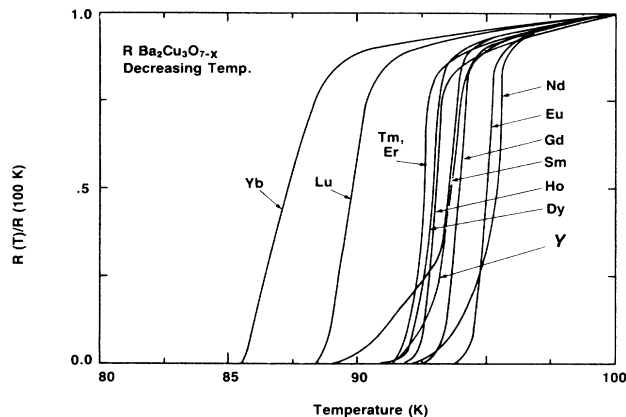


FIG. 6. Resistance vs temperature, normalized to the value at 100 K, is plotted from 100 K to below  $T_c$  for  $R\text{Ba}_2\text{Cu}_3\text{O}_{7-x}$ . These measurements were taken while decreasing the temperature at a rate of approximately 5 K/min using current densities of 0.1 to 0.5 A/cm.<sup>2</sup>

currents, but it is too early to state whether this is due to resistive loss at grain boundaries or is an intrinsic property of these materials.

To further confirm bulk superconductivity in these rare-earth perovskite phases, we measured the screening and exclusion of magnetic flux for several members of the series. The data for  $\text{NdBa}_2\text{Cu}_3\text{O}_{7-x}$  are shown in Fig. 7 as an example. For each sample, the Meissner effect was found to range between 30% to 50% of that expected for a perfect superconductor, while the Meissner-to-shielding ratio is on the order of 50%.

The effect of oxygen nonstoichiometry on the physical properties of the  $R$  compounds has been studied by resistivity and ac susceptibility measurements. From ac measurements no signature of superconductivity was observed for the vacuum-annealed  $R$  samples in contrast to a full signal for the materials reannealed under oxygen. Resistively, this is shown for  $\text{ErBa}_2\text{Cu}_3\text{O}_{7-x}$  in Fig. 8, where the resistivity from room temperature to below  $T_c$  is plot-

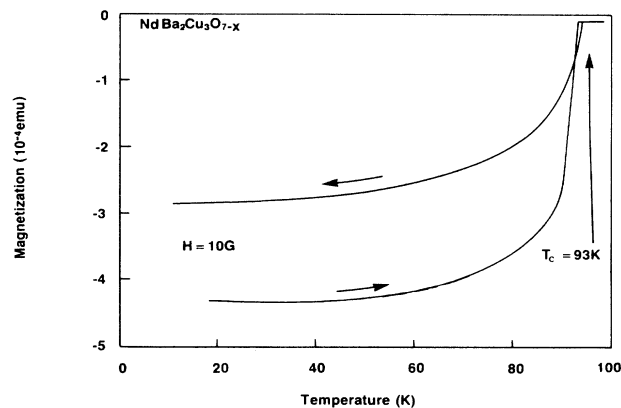


FIG. 7. Magnetic susceptibility vs temperature for  $\text{NdBa}_2\text{Cu}_3\text{O}_{7-x}$ . The upper curve is for cooling in a field of 10 G (Meissner); the lower curve is for warming in 10 G after cooling in zero field (shielding). The sample weight was 65 mg.

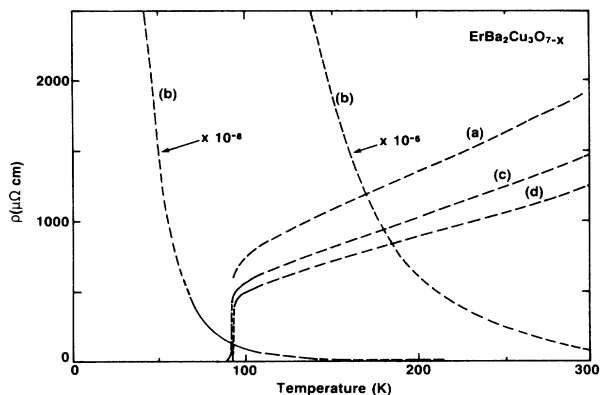


FIG. 8. Effect of oxygen on the transport properties of  $\text{ErBa}_2\text{Cu}_3\text{O}_{7-x}$ . Resistivity vs temperature is plotted from 300 to 30 K for the same sample; (a) as grown; (b) annealed in vacuum ( $10^{-3}$  Torr,  $420^\circ\text{C}$ , 12 h). (c) and (d) Reannealed in oxygen at  $720^\circ\text{C}$  under 1 and 40 atm of oxygen, respectively. Note the dramatic increase in resistivity for (b) plotted with two contracted scales of  $10^{-6}$  and  $10^{-8} \times \rho$ .

ted for the same sample (a) as grown, (b) vacuum annealed, (c) reannealed in oxygen, and (d) annealed in high pressure (40 bars) of oxygen. The striking feature of this graph is that the vacuum-annealed sample is a semiconductor (i.e., the resistivity increases with decreasing temperature). Note also that superconductivity can be fully recovered by reannealing the sample at  $720^\circ\text{C}$  under (c) oxygen. Further annealing in oxygen at higher pressure increases  $T_c$  by 1 K, but does not significantly affect the resistivity above  $T_c$ . This effect is considerably smaller than the increase of 30 K measured by Politis<sup>18</sup> on samples retreated under pressure of oxygen.

The ability to substitute yttrium, which is trivalent, by other rare earths strongly suggests that the  $R$  ions are trivalent in the compound. A simple way to check the

valence is to perform magnetic measurements. Figure 9 shows the inverse of the magnetic susceptibility as a function of the temperature (from above  $T_c$  to room temperature) for all the rare-earth compounds except Sm and Eu, which are van Vleck ions. Note that within this temperature range, all the compounds except Nd and Yb can be fit to a Curie-Weiss law for susceptibility,  $\chi = N\mu^2/3k_B(T - \Theta_p)$ . The effective magnetic moments ( $\mu$ ) and paramagnetic Curie temperatures ( $\Theta_p$ ) resulting from this fit are reported in Table II. For comparison, the theoretical effective moments for each free-trivalent ion are listed. Note the agreement between experimental and theoretical values. For the Nd and Yb compounds a deviation from the Curie-Weiss law is observed. A similar effect has previously been observed on the 40-K superconductors doped with Nd (Ref. 13) and has been attributed to the splitting of the rare-earth ions by the crystal field effect, which is generally larger for the lighter rare-earth ions. In the case of Yb the small amount of second phase detected by x-ray powder diffraction is likely responsible for the nonlinearity of the  $1/\chi$  vs  $T$  plot.

Another interesting result is that the paramagnetic Curie temperatures are negative (i.e., indicating that within this structure the magnetic rare-earth ions interact antiferromagnetically) and range from  $-35$  K for thulium to  $-2$  K for gadolinium. According to the  $\Theta_p$  values, if antiferromagnetic ordering should occur in these compounds it will be at low temperatures. To measure  $\chi$  down to low temperatures we destroyed superconductivity by annealing the samples under vacuum. The inverse susceptibility as a function of the temperature down to 1.6 K for several members of the rare-earth series is shown in Fig. 10. Note that a Curie-Weiss law is nearly perfectly obeyed from 10 to 300 K. The effective magnetic moment and paramagnetic Curie temperature deduced from this plot are similar to those already reported in Table II. Figure 10 shows the variation of the magnetic susceptibility as a function of temperature between 1.6 and 30 K. Except for

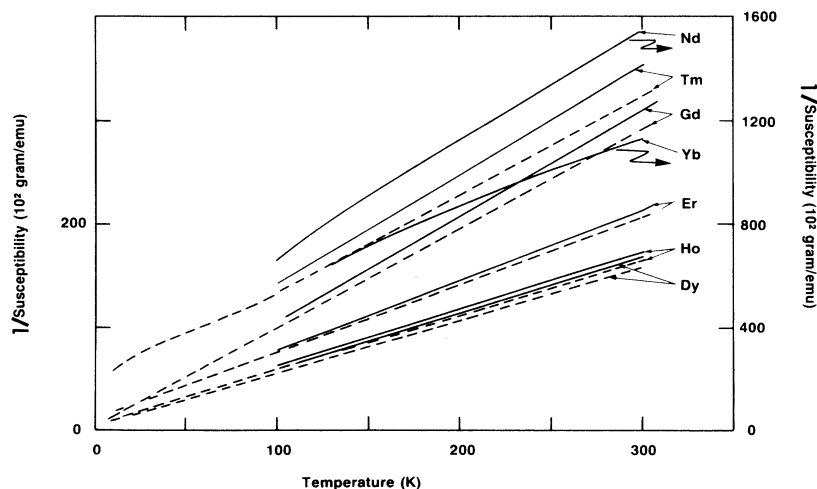


FIG. 9. Magnetic data collected at a field of 10 kG for the  $\text{RBa}_2\text{Cu}_3\text{O}_{7-x}$  series. The reciprocal susceptibility ( $\chi^{-1}$ ) is shown for the as-prepared samples (solid curve) and vacuum annealed samples (dashed curve) over the temperature range 100–300 K and 4–300 K, respectively.

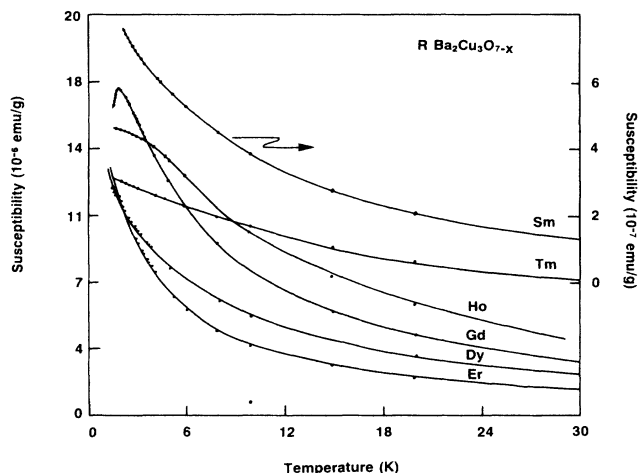


FIG. 10. The magnetic susceptibility in a magnetic field of 10 kG for the vacuum-annealed samples is plotted over the temperature range 1.6–30 K. The curves through the data points are a guide to the eye.

Ho and Gd, the susceptibility increases continuously with decreasing temperatures. For the Ho compound the susceptibility levels off around  $T=1.6$  K, suggesting the possibility of an antiferromagnetic ordering at lower temperatures. An important feature of Fig. 10 is that for the Gd compound, the susceptibility is going through a maximum near 2 K, indicating an antiferromagnetic ordering. Resistivity measurements show no reentrant behavior associated with this ordering. Fisk *et al.*<sup>19</sup> have reported a large anomaly in the heat-capacity measurements at 2.24 K for the gadolinium compound.

Figure 11 shows the susceptibility of the Gd vacuum

annealed compound from 1.6 to 300 K. The low-temperature part of the curve (inset) has been enlarged to emphasize the antiferromagnetic ordering occurring at 2.04 K. To ensure that the removal of oxygen from the starting material has no effect on antiferromagnetism we performed susceptibility measurements on the superconducting phase between 1.6 and 30 K at a field of 10 kG. The inset of Fig. 11 shows that the maximum susceptibility corresponding to an antiferromagnetic ordering ( $T_N=2.3$  K) is still present, suggesting the coexistence of superconductivity and antiferromagnetism.

At first sight it seems surprising to see a paramagnetic susceptibility in a superconductor. But the applied field (10 kG) here is much larger than  $H_{c1}$  ( $\approx 400$  G), so that much of the material is threaded by flux. Thus, the measured  $\chi$  is a combination of the paramagnetism of the normal part and the diamagnetism of the superconducting part of the sample. Because of the large moment of the Gd ions ( $8\mu_B$ ) the paramagnetic part dominates, but the diamagnetic part lowers the susceptibility from that in the vacuum-annealed sample, as observed experimentally (Fig. 11, inset).

The temperature-dependent susceptibility from 4 to 300 K for the vacuum annealed Eu, Sm, and Y compounds is shown in Fig. 12.  $\text{Eu}^{3+}$  ( $J=0$ ) is a van Vleck ion, so one would expect the susceptibility to remain constant up to 100 K and then decrease at higher temperatures, as observed in the rare-earth-doped La-Sr-Cu-O system.<sup>13</sup> The data do not confirm our expectations since the susceptibility strongly increases below 100 K instead of leveling off. A common reason to account for such effect is the presence of magnetic impurities. For example, Eu could act as a magnetic impurity on the Ba sites. Europium is one of the few rare earths which can exist under two oxidation states (2+ and 3+). Europium 2+ ( $J=+\frac{7}{2}$ ) is magnetic and furthermore has about the same ionic radius as

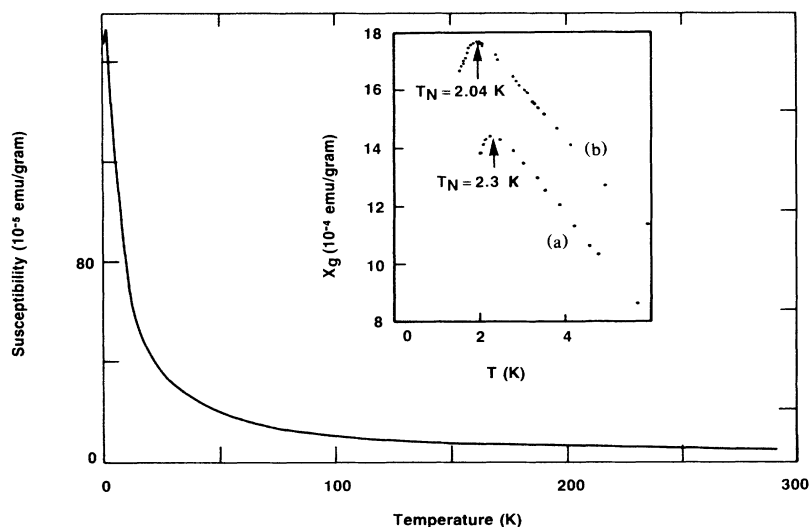


FIG. 11. The susceptibility in a magnetic field of 10 kG as a function of temperature is shown for  $\text{GdBa}_2\text{Cu}_3\text{O}_{7-x}$  over the temperature range 1.6–300 K. The inset is the enlargement of the low-temperature part for (a) the vacuum-annealed sample and (b) the as-grown sample.

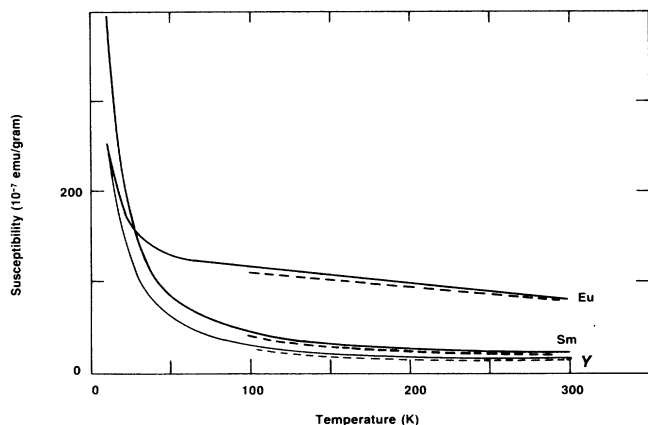


FIG. 12. The magnetic susceptibility as a function of the temperature is shown for the Eu, Sm, and Y compounds. Dashed curves refer to the as-grown samples and solid curves to the vacuum-annealed samples.

$\text{Ba}^{2+}$ . These results may suggest that compounds of general formula  $\text{EuBa}_{2-y}\text{Eu}_y\text{Cu}_3\text{O}_{7-x}$  exist.

#### DISCUSSION

Magnetic ions at first sight are expected to decrease  $T_c$ , because the exchange interactions between the rare-earth ion and the conduction electron destroys the Cooper pairs responsible for superconductivity. However, the resistivity in Fig. 6 shows that the superconducting critical temperature of the  $\text{YBa}_2\text{Cu}_3\text{O}_{7-x}$  phase does not significantly change when Y is replaced by trivalent rare-earth ions. This result indicates that the magnetic ions do not interact with the conduction electrons. The structure of these compounds consists of three perovskite layers, so that the yttrium atoms are separated by  $\text{CuO}_2$ ,  $\text{BaO}$ ,  $\text{CuO}_2$ ,  $\text{BaO}$ , and  $\text{CuO}_2$  planes. To reach the oxygen stoichiometry of seven, an oxygen atom is removed from the middle  $\text{CuO}_2$  layer. Within this layer the vacancies are ordered so that  $\text{CuO}$  chains running parallel to the  $b$  direction are formed. Band-structure calculations have been performed<sup>20</sup> on these materials and the main result is that the superconducting properties of these materials are governed by the  $\text{Cu-3d}$  and  $\text{O-2p}$  electrons. These calculations, however, do not indicate whether the superconducting electrons are in the copper plane or copper chains, or both. The insensitivity of  $T_c$  to the presence of magnetic rare-earth ions suggests that the superconducting electrons are far away from the magnetic ions, which is an argument that the copper-oxygen chains are responsible for superconductivity on these materials.

It is now of interest to compare the effect of rare-earth doping on both the 40- and 90-K superconductors. On the former ones we correlate a decrease of  $T_c$  by 20 K through the rare-earth series with a volume decrease due to the lanthanide contraction. For the 90-K compounds we also observed a volume decrease in going from the Nd to Yb compounds, but  $T_c$  remains nearly constant (within 3 K). The indifference of the superconducting properties of the

90-K perovskites with respect to volume contraction has also been observed by Hor *et al.*<sup>21</sup> who did not observe significant changes in  $T_c$  under applied pressure.

For a long time perovskite compounds have been intensively studied for their potential interest as oxygen sensors based on their ability to reversibly intercalate oxygen atoms. Thus, the great structural flexibility of the  $\text{RBa}_2\text{Cu}_3\text{O}_{7-x}$  perovskites to reversibly accommodate oxygen atoms is not surprising. In contrast, the superconducting to semiconducting transition induced by removal of oxygen in these materials is more intriguing. Changes in oxygen content imply changes in the oxidation states of copper atoms. The average valence of copper increases or decreases with the uptake or removal of oxygen atoms, respectively. With  $\text{YBa}_2\text{Cu}_3\text{O}_{7-x}$ , for example, we found that the oxygen content can change from 6.7 to 6.2 resulting in a change in the average valence of copper from 2.2 to 1.8. This valence implies the formation of  $\text{Cu}^{1+}$ . The shrinking of the  $b$  lattice parameter mentioned previously suggests that the oxygen atoms between the copper atoms are removed, so that copper which was fourfold coordinated becomes twofold coordinated with an oxygen above and below. In  $\text{Cu}_2\text{O}$  the monovalent copper ions are also bonded to two oxygen atoms. Thus it may be that the removal of oxygen atoms from the Cu-O chains changes the oxidation state of copper to  $1+$ . Recent neutron experiments have shown that vacuum annealing removes oxygen from the center Cu-O planes, but does not disturb the upper or lower Cu-O planes.<sup>22</sup> Since we have shown that vacuum annealing destroys superconductivity, we conclude that the presence of oxygen in the center Cu-O plane is required for superconductivity and put forth the argument that the superconducting transport occurs in the oxygen chains in the center Cu-O plane. X-ray photoemission spectroscopy measurements remain to be done in both annealed and vacuum-annealed samples to determine the predicted change in the valence of copper.

We turn now to the magnetism in these rare-earth perovskites. The data have shown that antiferromagnetism occurs only for the Gd compound, at least down to 1.6 K. If the rare-earth magnetic ions interacted via the Ruderman-Kittel-Kasuya-Yosida (RKKY) mechanism, which involves conduction electrons, one would expect from the Abrikosov and Gorkov theory<sup>23</sup> that the depression in  $T_c$  scales with the de Gennes factor  $G = (g_j - 1)^2 J(J + 1)$ , which is maximum for Gd. In the same way, magnetic transitions should also scale with  $G$ . The data show that the magnetic ordering temperature is maximum for Gd, but no depression in  $T_c$  was observed for this compound. We thus conclude that the RKKY interactions are not predominant in this system. Another type of magnetic interaction that we might consider in a system which orders at such a low temperature is dipole-dipole interactions. For instance Redi and Anderson<sup>24</sup> have shown that antiferromagnetism can result from such an interaction. The magnetic dipole-dipole interaction and the magnetic ordering temperature should depend on the total angular momentum  $J$ , which is largest for Tm, not Gd. But the orbital part  $L$  may constrain the moment to lie in an unfavorable direction for the magnetic ordering to occur. Thus, the magnetic transition may be

highest for Gd because it has  $L = 0$  (isotropic), so that it is unaffected by the crystal anisotropy.

In summary we have shown that the replacement of yttrium by rare-earth magnetic ions in  $\text{YBa}_2\text{Cu}_3\text{O}_{7-x}$  does not significantly affect the superconducting properties of these materials. The large amount of magnetic ions in this structure (8%) favors the possibility of magnetic structure as shown for the Gd compound [antiferromagnetic ordering at ( $T_N = 2.3$  K)]. In contrast we found that the electrical properties of these materials strongly depend on their processing because of their great ability to rever-

sibly intercalate oxygen. Superconductivity can be destroyed or recovered by annealing these materials under vacuum or oxygen, respectively.

#### ACKNOWLEDGMENTS

We wish to thank W. L. Feldman for technical assistance and P. W. Anderson, G. Baskaran, B. Bagley, W. Bonner, J. Greedan, Y. Le Page, J. Rowell, and J. Wernick for helpful discussions.

\*Permanent address: Division of Chemistry, National Research Council of Canada, Ottawa, Canada K1A0R9.

- <sup>1</sup>J. G. Bednorz and K. A. Müller, *Z. Phys.* **B 64**, 189 (1986).
- <sup>2</sup>J. G. Bednorz, M. Takashige and K. A. Müller, *Europhys. Lett.* **3**, 379 (1987).
- <sup>3</sup>S. Uchida, H. Takagi, K. Kitazawa, and S. Tanaka, *Jpn. J. Appl. Phys. Lett.* **26**, 21 (1987).
- <sup>4</sup>K. Kishio, K. Kitazawa, S. Kanbe, I. Yasuda, N. Sugii, H. Takagi, S. Uchida, K. Fueki, and S. Tanaka, *Chem. Lett.* (to be published).
- <sup>5</sup>R. J. Cava, R. B. van Dover, B. Batlogg, and E. A. Rietman, *Phys. Rev. Lett.* **58**, 408 (1987).
- <sup>6</sup>J. M. Tarascon, L. H. Greene, W. R. McKinnon, G. W. Hull, and T. H. Geballe, *Science* **235**, 1373 (1987).
- <sup>7</sup>M. K. Wu, J. R. Ashburn, C. J. Torng, P. H. Hor, R. L. Meng, L. Gao, Z. J. Huang, Y. Q. Wang, and C. W. Chu, *Phys. Rev. Lett.* **58**, 908 (1987).
- <sup>8</sup>J. M. Tarascon, L. H. Greene, W. R. McKinnon and G. W. Hull, *Phys. Rev. B* **35**, 7115 (1987).
- <sup>9</sup>Y. Le Page, W. R. McKinnon, J. M. Tarascon, L. H. Greene, G. W. Hull, and D. M. Hwang, *Phys. Rev. B* **35**, 7245 (1987).
- <sup>10</sup>R. J. Cava, B. Batlogg, R. B. van Dover, D. W. Murphy, S. Sunshine, T. Siegrist, J. P. Remeika, E. A. Rietman, S. Zahurak, and G. Espinosa, *Phys. Rev. Lett.* **58**, 1676 (1987); T. Siegrist, S. Sunshine, D. W. Murphy, R. J. Cava, and S. M. Zahurak, *Phys. Rev. B* **35**, 7137 (1987).
- <sup>11</sup>P. M. Grant, R. B. Beyers, E. M. Engler, G. Lim, S. S. P. Parkin, M. L. Ramirez, V. Y. Lee, A. Nazzal, J. E. Vazquez, and R. J. Savoy, *Phys. Rev. B* **35**, 7242 (1987).
- <sup>12</sup>J. E. Greedan, A. O'Reilly, and C. V. Stager, *Phys. Rev. B* **35**, 8770 (1987).
- <sup>13</sup>J. M. Tarascon, L. H. Greene, W. R. McKinnon, and G. W. Hull, *Solid State Commun.* **63**, 499 (1987).
- <sup>14</sup>Z. Fisk, J. D. Thompson, E. Zirngiebl, J. L. Smith, and S. W. Cheong, *Solid State Commun.* (to be published).
- <sup>15</sup>H. Takagi, S. Uchida, H. Sato, H. Ishii, K. Kishio, K. Kitazawa, K. Fueki, and S. Tanaka, *Jpn. J. Appl. Phys.* (to be published).
- <sup>16</sup>D. W. Murphy, S. Sunshine, R. B. van Dover, R. J. Cava, B. Batlogg, S. M. Zahurak, and L. F. Schneemeyer, *Phys. Rev. Lett.* **58**, 1888 (1987).
- <sup>17</sup>W. R. McKinnon, J. M. Tarascon, L. H. Greene, and G. W. Hull (unpublished).
- <sup>18</sup>C. Politis, postdeadline paper presented at the Meeting of the American Physical Society, New York, March 1987 (unpublished).
- <sup>19</sup>Z. Fisk, J. O. Willis, J. D. Thompson, S. W. Cheong, J. L. Smith, and E. Zirngiebl (unpublished).
- <sup>20</sup>L. F. Mattheis and D. R. Hamann (unpublished).
- <sup>21</sup>P. H. Hor, L. Gao, R. L. Meng, Z. J. Huang, Y. Q. Wang, K. Forster, J. Vassiliou, C. W. Chu, M. K. Wu, J. R. Ashburn, and C. J. Torng, *Phys. Rev. Lett.* **58**, 911 (1987).
- <sup>22</sup>J. E. Greedan, A. O'Reilly and C. V. Stager (unpublished).
- <sup>23</sup>A. A. Abrikosov and L. P. Gorkov, *Zh. Eksp. Teor. Fiz.* **39**, 1781 (1960) [*Sov. Phys. JETP* **12**, 1243 (1961)].
- <sup>24</sup>M. Redi and P. W. Anderson, *Proc. Nat. Acad. Sci. U.S.A.* **78**, 27 (1981).